Neuro-Oncology

The impact of coexisting genetic mutations on murine optic glioma biology

Aparna Kaul, Joseph A. Toonen, Scott M. Gianino, and David H. Gutmann

Department of Neurology, Washington University School of Medicine, St. Louis, Missouri

Corresponding Author: David H. Gutmann, MD, PhD, Department of Neurology, Washington University School of Medicine, Box 8111, 660 S. Euclid Avenue, St. Louis, MO 63110 (gutmannd@neuro.wustl.edu).

Background. Children with the neurofibromatosis type 1 (NF1) tumor predisposition syndrome are prone to the development of optic pathway gliomas resulting from biallelic inactivation of the *NF1* gene. Recent studies have revealed the presence of other molecular alterations in a small portion of these NF1-associated brain tumors. The purpose of this study was to leverage *Nf1* genetically engineered mouse strains to define the functional significance of these changes to optic glioma biology.

Methods. *Nf1*+/− mice were intercrossed with *Nf1*$^{flox/flox}$ mice, which were then crossed with *Nf1*$^{flox/flox}$; GFAP-Cre mice, to generate *Nf1*$^{flox/mut}$; GFAP-Cre (FMC) mice. These mice were additionally mated with conditional *KIAA1549:BRAF* knock-in or *Pten*$^{flox/wt}$ mice to generate *Nf1*$^{flox/mut}$; *f-BRAF*; GFAP-Cre (FMBC) mice or *Nf1*$^{flox/mut}$; *Pten*$^{flox/wt}$; GFAP-Cre (FMPC) mice, respectively. The resulting optic gliomas were analyzed for changes in tumor volume, proliferation, and retinal ganglion cell loss.

Results. While *KIAA1549:BRAF* conferred no additional biological properties on *Nf1* optic glioma, FMPC mice had larger optic gliomas with greater proliferative indices and microglial infiltration. In addition, all 3 *Nf1* murine optic glioma strains exhibited reduced retinal ganglion cell survival and numbers; however, FMPC mice had greater retinal nerve fiber layer thinning near the optic head relative to FMC and FMBC mice.

Conclusions. Collectively, these experiments demonstrate genetic cooperativity between *Nf1* loss and *Pten* heterozygosity relevant to optic glioma biology and further underscore the value of employing genetically engineered mouse strains to define the contribution of discovered molecular alterations to brain tumor pathogenesis.

Keywords: BRAF, neurofibromatosis, neurofibromin, pediatric brain tumor, PTEN.

Neurofibromatosis type 1 (NF1) is one of the most common genetic etiologies for pediatric brain tumors.[1,2] As such, 15%–20% of children with NF1 develop low-grade glial neoplasms (pilocytic astrocytomas [PAs]) arising along the optic pathway (optic nerve, chiasm, and postchiasmal tracts; optic pathway glioma [OPG]).[3,4] In some children with these NF1-OPGs, there may also be associated visual impairment[5,6] or hypothalamic dysfunction.[7] Since surgery and radiation therapy are not used due to the risk of permanent nerve damage and secondary malignancy,[8] respectively, the treatment of NF1-OPG has largely employed agents (vincristine and carboplatin) in routine use for sporadic low-grade glioma.[9,10]

Because NF1-OPGs are rarely biopsied for pathological diagnosis, there have been few analyses of the molecular changes that drive tumorigenesis in this condition. Immunohistochemical and whole genome (NexGen) sequencing studies have demonstrated biallelic inactivation of both *NF1* genes,[11] resulting in loss of NF1

protein (neurofibromin) expression in these NF1-associated brain tumors.[12,13] To model the human condition in which children with NF1 are born with one functional and one nonfunctional (germline *NF1* gene mutation) copy of the *NF1* gene, *Nf1*+/− mice with biallelic astroglial progenitor *Nf1* gene loss were generated.[14,15] These mice develop low-grade gliomas of the prechiasmatic optic nerves and chiasm with many similarities to their human counterparts.[14,16,17] As observed in human NF1-OPGs, these murine optic gliomas have low proliferative indices, increased microglia infiltration, and bipolar neoplastic glial cells with nuclear pleiomorphism and cellular atypia.[14,16,17]

While complete *NF1* gene inactivation is the rule for NF1-PA tumors, recent studies have revealed the presence of additional molecular changes in NF1-OPGs.[18,19] In some of these NF1-OPGs, heterozygous *PTEN* deletion (1/4 tumors) and *KIAA1549:BRAF* duplication (1/4 tumors) were detected, raising the intriguing possibility that genetic cooperativity between these molecular

alterations and neurofibromin loss might lead to more biologically aggressive tumors. To address this clinically relevant issue, we generated *Nf1* genetically engineered mouse (GEM) strains that harbor *Pten* reduction or *KIAA1549:BRAF* expression in addition to *Nf1* gene loss in neuroglial progenitors in vivo. Using these novel strains, we demonstrated that heterozygous *Pten* loss, but not *KIAA1549:BRAF* expression, cooperates with *Nf1* gene inactivation to increase murine optic glioma growth and retinal nerve defects.

Materials and Methods

Mice

Nf1^{flox/mut}; GFAP-Cre (FMC) mice (*Nf1*+/− mice with *Nf1* gene inactivation in neuroglial progenitors) were generated as previously described.[14] *Nf1*^{flox/mut} mice were intercrossed with *Lox-Stop-Lox* (LSL)-KIAA1549:BRAF (*LSL-f-BRAF*) mice,[20] and the resulting progeny were mated with *Nf1*^{flox/flox}; GFAP-Cre mice[21] to generate *Nf1*^{flox/mut}; *f-BRAF*; GFAP-Cre mice (FMBC mice). *Pten*^{flox/flox} mice[22] were intercrossed with *Nf1*^{flox/flox}; GFAP-Cre mice to generate *Pten*^{flox/wt}; *Nf1*^{flox/flox};GFAP-Cre mice. The resulting mice were then mated with *Nf1*^{flox/mut} mice to generate *Nf1*^{flox/mut}; *Pten*^{flox/wt}; GFAP-Cre (FMPC) mice. *LSL-f-BRAF* mice were crossed with GFAP-Cre mice to generate *f-BRAF*; GFAP-Cre mice (*f-BRAF*^{GFAP}).[20] All mice were maintained on a C57Bl/6 background and used in accordance with approved animal studies protocols at the Washington University School of Medicine.

Primary Astrocyte Cultures

Primary astrocyte cultures were established from the brainstems of postnatal day1–2 *Nf1*^{flox/flox}, *Pten*^{flox/wt} or *Nf1*^{flox/flox}; *Pten*^{flox/wt} mouse pups, as described previously.[23] Wild-type (WT) cultures were generated following infection with adenovirus type 5 containing β-galactosidase (Ad5-LacZ; University of Iowa Gene Transfer Vector Core), while *Nf1*−/−, *Pten*+/−, and *Nf1*−/−; *Pten*+/− cultures were generated following infection of *Nf1*^{flox/flox}, *Pten*^{flox/wt}, or *Nf1*^{flox/flox}; *Pten*^{flox/wt} cultures, respectively, with adenovirus type 5 containing Cre recombinase (Ad5-Cre). Astrocyte proliferation was assessed using the BrdU Cell Proliferation ELISA kit (Roche) according to the manufacturer's instructions.[20]

Western Blotting

Cells were lysed in buffer containing 1% NP-40, supplemented with protease and phosphatase inhibitors. Western blotting was performed as described previously[24] using the following antibodies: PTEN, AKT, pAKT^{T308} (Cell Signaling Technology), and α-tubulin (Sigma). Chemiluminescence signal was detected using the ChemiDoc-It Imaging System (UVP) and quantified using Visionworks software (UVP). Immunoblot signals from phosphorylated AKT (pAKT^{T308}) were normalized to total AKT to calculate relative AKT activation.

RNA Extraction and Real-time PCR

RNA was isolated from mouse optic nerves using Trizol reagent (Life Technologies) following the manufacturer's protocol. Total RNA was employed for cDNA synthesis using the SuperScript III first-strand synthesis system (Life Technologies).

The following primers were used for real-time (RT-PCR): *β-actin* 5′-GCTCGTCGTCGACAACGGCTC-3′ and 5′-CAAACATGATCTGGGTCA TCTTCTC-3′; *f-BRAF* 5′-CTTCCCAGGAAGAGAGGGGA-3′ and 5′-GA TGACTTCCTTTCTCGCTGAGGT-3′.[25,26]

Optic Nerve Measurements

Optic nerves with an intact chiasm were microdissected and photographed, and the optic nerve diameters were measured at the chiasm (∼150, ∼300, and ∼450 microns anterior to the chiasm) to generate optic nerve volumes, as previously reported.[27]

Immunohistochemistry

Murine eyes and optic nerves were prepared for sectioning and immunostaining as previously described.[28] The following primary antibodies were used for immunostaining: Brn3a (Santa Cruz), SMI-32 (Covance), GFP (Abcam), Pten (Cell Signaling), GFAP (Millipore), Ki67 (Abcam), and Iba1 (Wako). For immunohistochemistry on paraffin sections, biotinylated secondary antibodies (Vector Laboratories) were used in combination with Vectastain Elite ABC kit and developed with 3,3′-diaminobenzidine peroxidase substrate kit and hematoxylin counterstaining. For fluorescence-based detection, species-appropriate Alexa-Fluor-conjugated (Invitrogen) secondary antibodies were used, followed by DAPI counterstaining. Amplification of the Brn3a antibody signal was performed using a biotinylated secondary antibody, followed by HRP conjugation using Vectastain Elite ABC kit, and the fluorescent signal was amplified with Tyramide Signal Amplification Plus Cyanine 3 system (Perkin-Elmer) according to the manufacturer's instructions. Terminal deoxynucleotide transferase-mediated dUTP nick-end labeling (TUNEL) staining was performed using the ApopTag Plus in situ apoptosis fluorescein detection kit (Millipore) according to the manufacturer's recommendations.

Manganese-enhanced MRI

MRI imaging to visualize the optic nerves in mice was performed as described previously.[27]

Retinal Analyses

Quantitation of TUNEL⁺ cells was performed by counting the number of cells positive for TUNEL staining as a percentage of the total number of DAPI⁺ cells in the retinal ganglion cell layer. The total number of Brn3a⁺ cells was counted per section and normalized to control mice (set at 100%). Measurements of the retinal nerve fiber layer (RNFL) were performed following SMI-32 immunohistochemical staining using Image J software. Briefly, overlapping high-power images were taken at incremental distances from the optic nerve (−1,1: 0–250 μm; −2, 2: 250–500 μm; −3, 3: 500–750 μm; −4, 4: 750–1000 μm; and −5, 5: <1000 μm). Repeated measurements of the width of the stained axons (SMI-32⁺ staining) were recorded and averaged for each area. All quantitation was performed on sections through the optic nerve for a cohort of mice ($n = 3$) corresponding to each genotype.

Statistical Analysis

Data were analyzed using GraphPad Prizm 5.0 software using 2-way ANOVA for RNFL measurement data and Student *t* test for all other data comparisons with statistical significance set at $P < .05$. Scatter plot analysis examining the correlation between RNFL thickness and retinal ganglion cell (RGC) apoptosis was constructed using linear regression methods to generate the R^2 value in GraphPad Prizm 5.0 software.

Results and Discussion

The *KIAA1549:BRAF* rearrangement represents the signature genetic alteration observed in 50%–75% of sporadic PAs, in which the kinase domain of the *BRAF* gene is fused to the amino terminal exons of the *KIAA1549* gene.[29,30] The novel fusion protein generated by this molecular event (*fusion-BRAF; f-BRAF*) is hypothesized to create a molecule with constitutive BRAF kinase
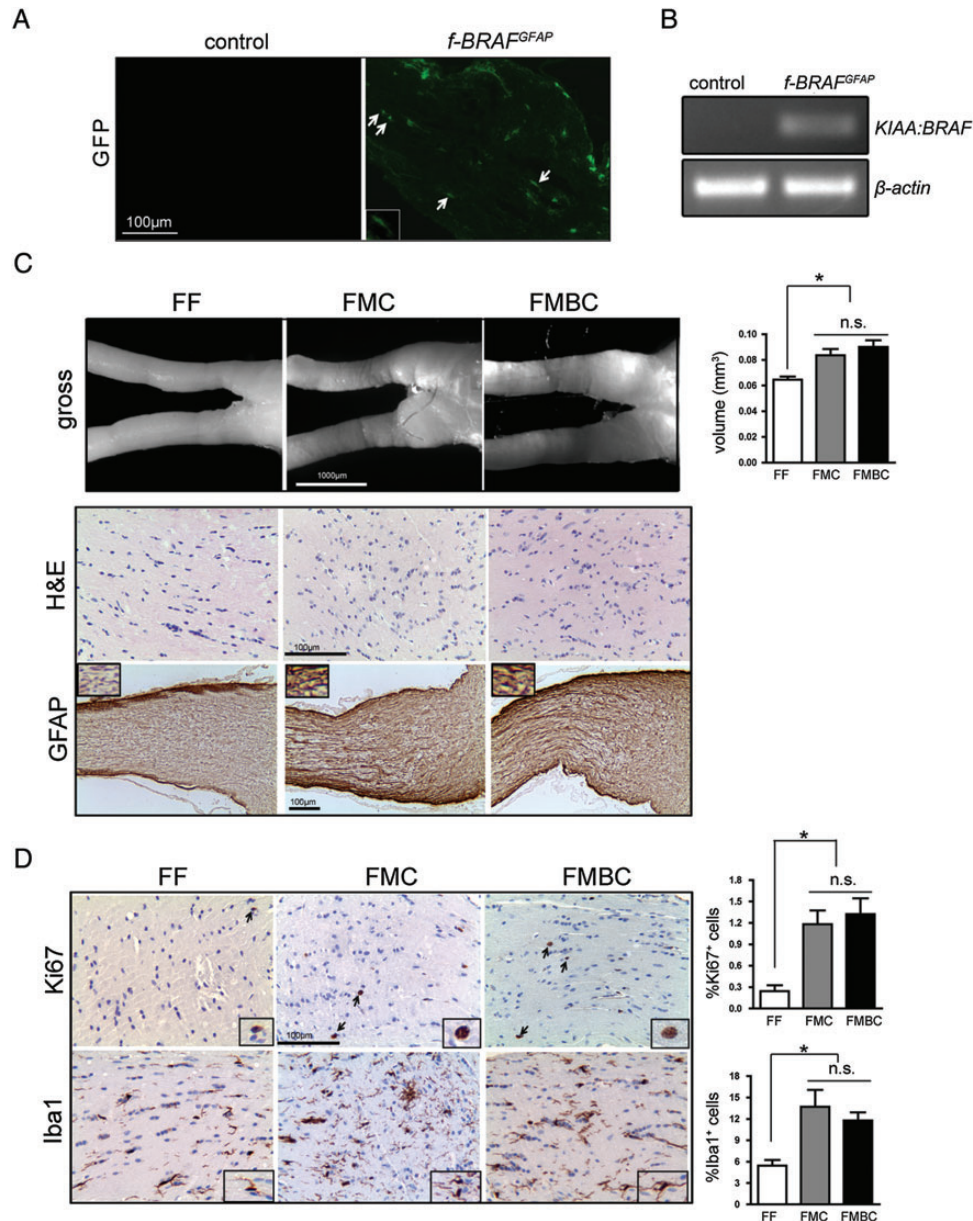

Fig. 1. *KIAA1549:BRAF* does not cooperate with *Nf1* loss in murine optic glioma. (A) Immunostaining demonstrates *f-BRAF* transgene (GFP, green) expression in *f-BRAF*^GFAP mouse optic nerves relative to controls. (B) Representative RNA real-time PCR confirms the presence of the *f-BRAF* transcript in the optic nerves of *f-BRAF*^GFAP mice. (C) No changes in optic nerve volume (gross, bar graph), GFAP expression, or cellularity (H&E) were observed in *Nf1*^flox/mut; *f-BRAF*; GFAP-Cre (FMBC) mouse optic nerves relative to littermate *Nf1*^flox/mut; GFAP-Cre (FMC) mice at 3 months of age. (D) Similarly, no changes in microglia content (%Iba1+ cells, bar graph) or proliferation (%Ki67+ cells, bar graph) were observed in FMBC mouse optic nerves relative to littermate FMC mice. *Nf1*^flox/flox (FF) mice were used as wild-type controls. Bar graph denotes mean ± SEM. Scale bar, as indicated. Arrows and insets depict representative immunopositive cells. (*) $P < .05$. n.s., not significant.

activity.[29,31] To determine the contribution of *KIAA1549:BRAF* (f-BRAF) to *Nf1* murine optic glioma pathogenesis, *Nf1+/−* mice were generated that conditionally express f-BRAF and lack *Nf1* expression in neuroglial cells (*Nf1*$^{flox/mut}$; *f-BRAF*; GFAP-Cre mice, FMBC mice) using the human GFAP-Cre transgenic mouse line.[25] Since antibody reagents do not exist to detect the *KIAA1549:BRAF* protein, we verified *KIAA1549:BRAF* transgene expression in the optic nerves by 2 different methods. First, we leveraged the green fluorescent protein (GFP) gene engineered into the *KIAA1549:BRAF* Rosa26 locus targeting vector as a surrogate marker of *KIAA1549:BRAF* transgene expression. GFP+ cells were detected in the optic nerves of 1-month-old *f-BRAF*; GFAP-Cre (*f-BRAF*^{GFAP}) mice (Fig. 1A). Second, the presence of the *f-BRAF* transcript was demonstrated in the optic nerves of *f-BRAF*^{GFAP} mice by RNA RT-PCR using previously published primers.[25,26] (Fig. 1B).

Despite robust *KIAA1549:BRAF* transgene expression, the optic nerves of FMBC mice (n = 9) were indistinguishable from their FMC counterparts (n = 8) with respect to optic nerve volume, GFAP expression, or histopathological appearance (H&E staining; Fig. 1C) at 3 months of age. Similarly, microglia numbers (%Iba1+ cells) and proliferative indices (%Ki67+ cells) were similar to those observed in FMC optic nerves (Fig. 1D). These results indicate that *KIAA1549:BRAF* expression does not confer any additional biological properties on murine *Nf1* glioma growth.

Next, we sought to determine whether heterozygous *Pten* gene loss could synergize with *Nf1* loss. For these studies, we generated *Nf1+/−* mice with both absent *Nf1* gene expression and reduced *Pten* gene expression in neuroglial progenitors (*Nf1*$^{flox/mut}$; *Pten*$^{flox/wt}$; GFAP-Cre mice, FMPC mice). As expected, Pten expression was reduced, but not absent, in the optic nerves of FMPC mice relative to FMC optic nerves as revealed by
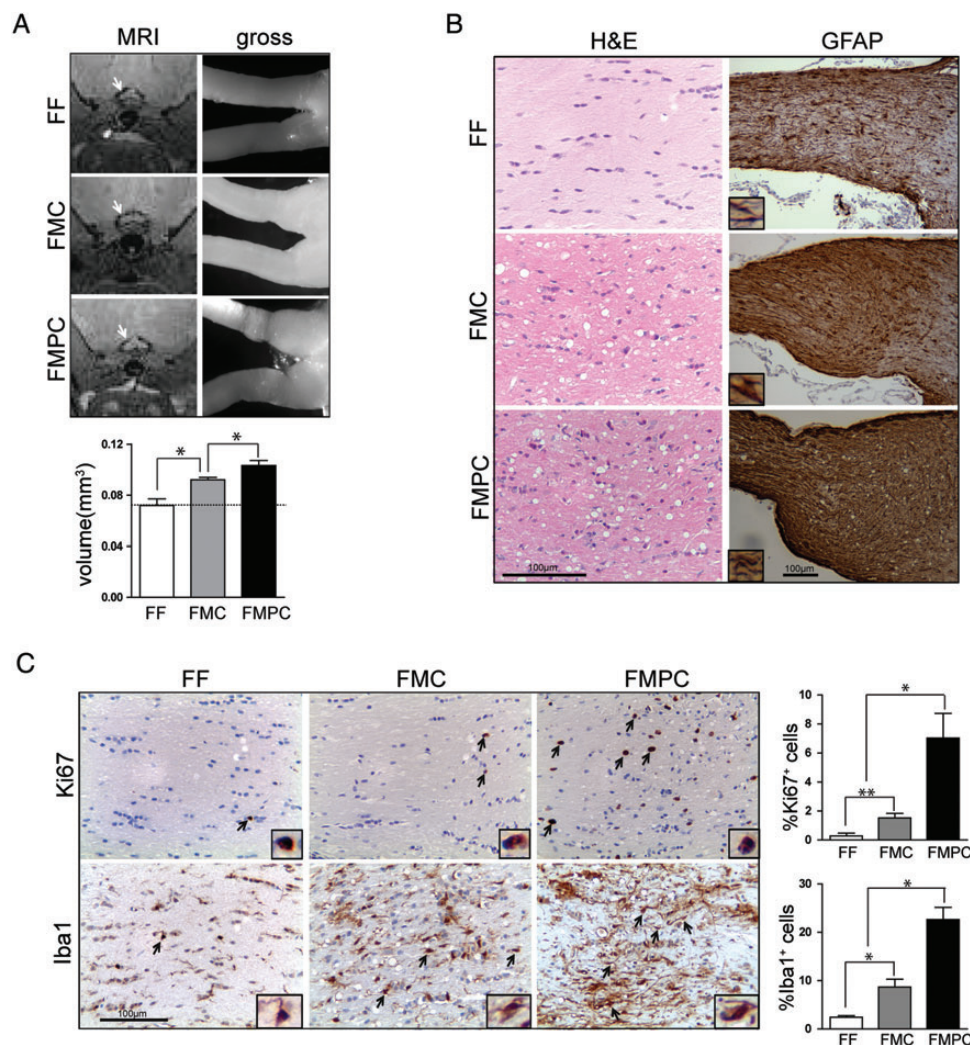
Fig. 2. Heterozygous *Pten* loss cooperates with *Nf1* loss in murine optic glioma. (A) *Nf1*$^{flox/mut}$; *Pten*$^{flox/wt}$; GFAP-Cre (FMPC) mice exhibit increased optic nerve volumes on both MRI and gross histological appearance at 3 months of age. (B) Increased cellularity (H&E) and increased GFAP immunoreactivity were observed in FMPC optic nerves relative to FMC mice. (C) FMPC optic nerves have increased percentages of Ki67+ and Iba1+ cells relative to FMC mice. *Nf1*$^{flox/flox}$ (FF) mice were used as wild-type controls. (*) $P < .01$, (**) $P < .05$. Bar graph denotes mean ± SEM. Scale bar, 100 μm. Arrows and insets denote representative immunopositive cells.
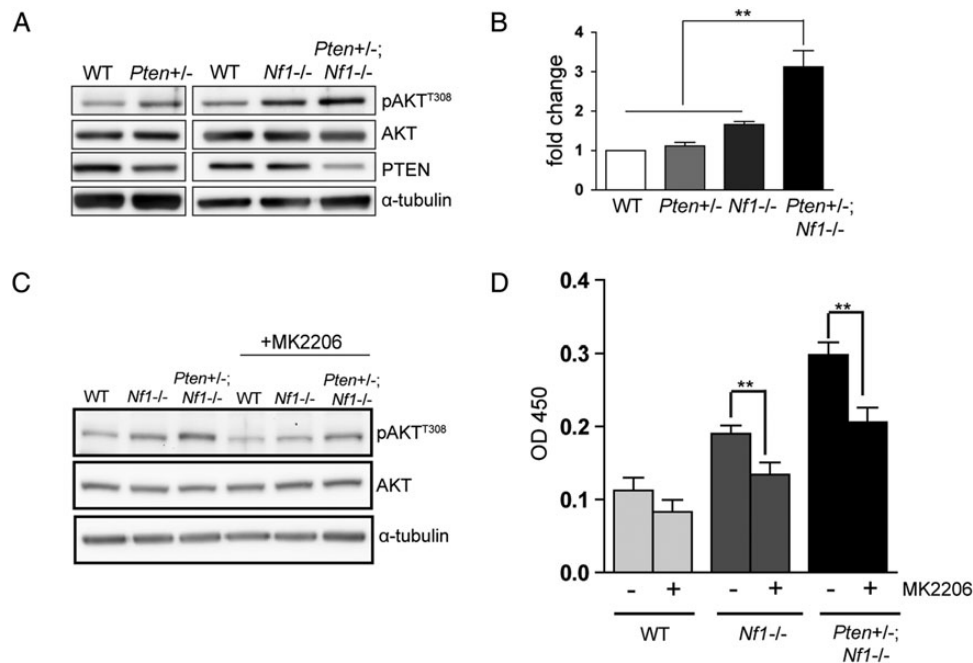
Fig. 3. PI3K pathway activation synergizes with *Nf1* loss to increase murine astrocyte proliferation. (A) Western blot demonstrates increased AKT phosphorylation (pAKT^{T308}) in *Pten*+/− and *Nf1*−/− astrocytes, which is further increased in *Pten*+/−; *Nf1*−/− astrocytes. Tubulin was used as an internal control for equal protein loading. (B) Bar graph reveals a synergistic increase in astrocyte proliferation in *Pten*+/−; *Nf1*−/− astrocytes relative to *Pten*+/− or *Nf1*−/− astrocytes. The fold changes were normalized to *Nf1*$^{flox/flox}$ (WT) astrocytes. Treatment with 50nM MK2206 inhibited the increased (C) AKT activation (AKT^{T308} phosphorylation) and (D) proliferation observed in *Nf1*−/− astrocytes and *Pten*+/−; *Nf1*−/− astrocytes. (**) $P < .05$. Bar graph denotes mean ± SEM.

immunohistochemistry (Supplementary material, Fig. S1A). Similar to their FMC counterparts, focal enlargements of the optic nerves and chiasm were observed in all FMPC mice by small-animal MRI (Fig. 2A) at 3 months of age. However, the optic nerves of FMPC mice ($n = 9$) were larger when compared with FMC mice. In FMPC mice, we observed a 12% increase in nerve optic nerve volumes relative to FMC mice. When considering only the volume contributed by the tumor (after subtracting the volume of the normal nerves in FF control mice), FMPC mice exhibited a 55% increase in tumor volume compared with FMC mice (Fig. 2A, volume above the dotted line in the bar graph). In addition, these FMPC optic gliomas contained striking hypercellularity, increased numbers of atypical cells (H&E staining), and higher GFAP immunoreactivity relative to FMC mice (Fig. 2B). Furthermore, there was a 4.6-fold increase in the percent of proliferating (Ki67^{+}) cells and a 2.6-fold increase in the percent of infiltrating Iba1^{+} microglia in FMPC mice compared with FMC mice (Fig. 2C). These findings demonstrate that *Pten* reduction cooperates with neurofibromin loss to increase *Nf1* murine optic glioma growth in vivo.

The observation that *Pten* haploinsufficiency can impact NF1-associated tumor biology is further supported by GEM studies demonstrating that reduced *Pten* gene expression accelerates benign neurofibroma formation and malignant progression[32,33] as well as the development of high-grade astrocytomas resulting from combined *Nf1* and *p53* gene inactivation[34] in mice. This cooperative effect likely reflects the activation of a common downstream growth regulatory effector (AKT). As such, while reduced *Pten* expression or *Nf1* loss in primary

astrocytes resulted in 1.5-fold and 2-fold increases in AKT activation (T308 phosphorylation), respectively, combined *Nf1* loss and Pten reduction led to a 3-fold increase in AKT phosphorylation (Fig. 3A). Similarly, whereas *Pten* reduction alone had no effect on astrocyte proliferation, *Nf1* loss resulted in a 1.7-fold increase in proliferation, and astrocytes with both *Nf1* loss and Pten reduction exhibited a 3-fold increase in proliferation (Fig. 3B).

To determine whether Pten reduction increases *Nf1*-deficient astrocyte proliferation and optic glioma growth in an mTOR-dependent manner, we performed a series of experiments. First, inhibition of AKT activity using the MK2206 compound (50nM) suppressed both *Nf1*-deficient and *Nf1*−/−;*Pten*+/− astrocyte proliferation in vitro (Fig. 3C and D). This inhibition of *Nf1*-deficient astrocyte proliferation is consistent with previous reports from our laboratory demonstrating that mTOR hyperactivation following neurofibromin loss requires AKT activity.[35,36]

To determine whether this cooperativity reflects convergence on mTOR, we measured mTOR activation as assessed by ribosomal S6 phosphorylation. Interestingly, there were no further increases in S6 phosphorylation in *Nf1*−/−;*Pten*+/− astrocytes in vitro or FMPC optic gliomas in vivo compared with *Nf1*-deficient astrocytes or FMC tumors, respectively (Supplementary material, Fig. S1B and C). Since ribosomal S6 represents only one of many mTOR effectors, we examined the activation (phosphorylation status) of both mTOR complex 1 (C1) and complex 2 (C2) molecules. As observed with S6, no further increases were observed in mTORC1 (4E-BP1, PRAS40) or mTORC2 (AKT^{S473}, PKCα) effector activation (Supplementary material, Fig. S1C). Taken together, these observations indicated that Pten heterozygosity likely
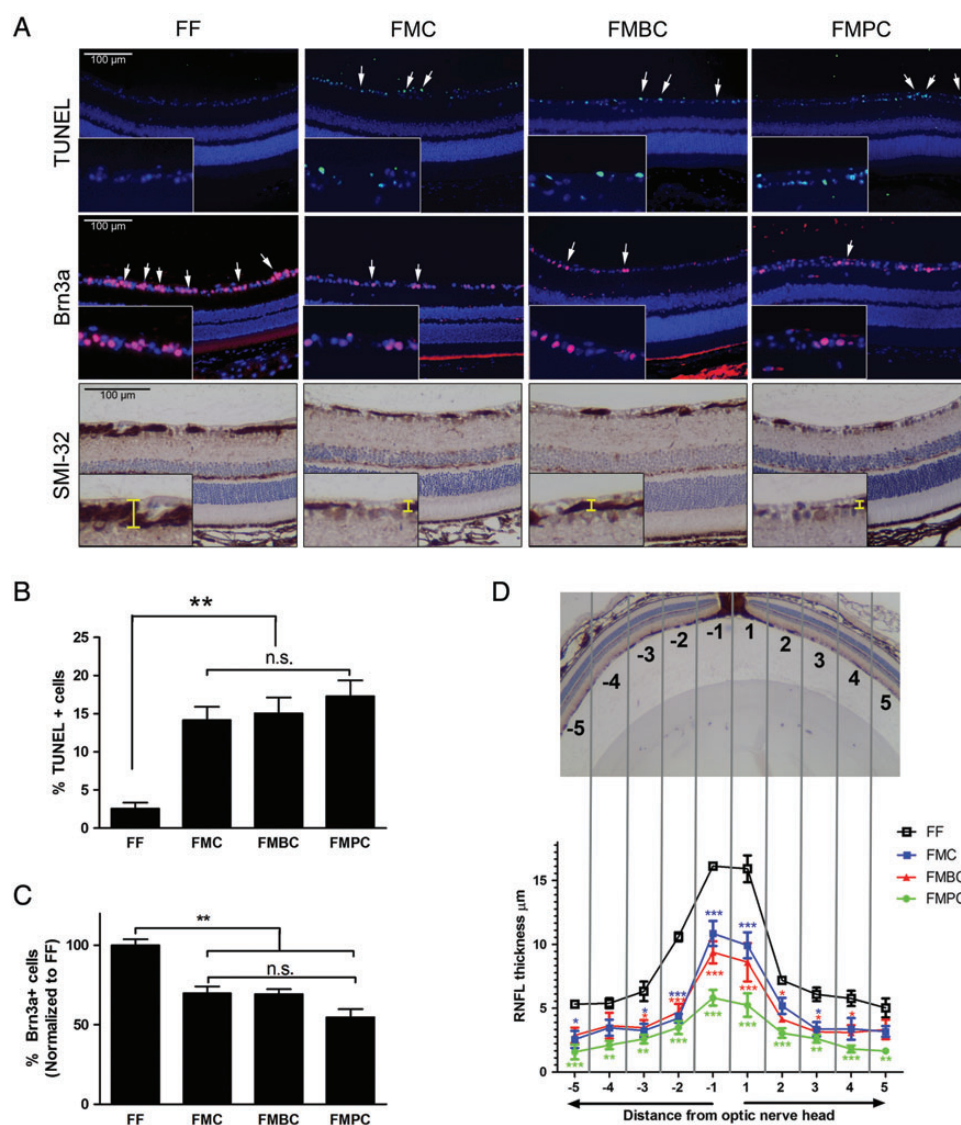
Fig. 4. Increased retinal ganglion cell dysfunction accompanies optic glioma formation in *Nf1* mutant mice. (A) TUNEL staining (top panels), immunohistochemistry using Brn3a (middle panels), and SMI-32 (lower panels) reveal increased apoptosis (TUNEL$^+$ cells; arrows), retinal ganglion cell loss (Brn3a$^+$ cells, arrows), and retinal nerve fiber layer thickness (RNFL; SMI-32) in FMC, FMBC, and FMPC mice relative to FF control mice. The insets illustrate individual TUNEL$^+$ (top panels) and Brn3a$^+$ (middle panels) cells, whereas the insets in the lower panels demonstrate the RNFL thickness (yellow brackets). The percent of TUNEL$^+$ and Brn3a$^+$ cells are quantified in panels B and C, respectively. (D) Quantitation of the RNFL thickness as a function of the distance from the optic nerve head is illustrated above and graphically represented below. Scale bars, 100 μm; *, $P <$ .05; **$P <$ .01 ***, $P <$ .001; n.s., not significant.

functions in an mTOR-independent manner to synergize with neurofibromin loss in the pathogenesis of NF1-OPG. These findings suggest that combinatorial therapy targeting both PI3K and mTOR may be useful in a subset of NF1-associated optic gliomas, similar to high-grade gliomas.[37,38] Current studies using a combination of approaches are in progress to identify potential effectors that operate downstream of PTEN/PI3-Kinase.

Children with NF1-OPG often come to medical attention because of reduced visual function.[5,39] Since these tumors arise in young preverbal children, it is often challenging to accurately assess their visual acuity, especially when compounded with behavioral and attention deficits common in this patient population.[40–42] To circumvent these problems, objective measures have been sought. One of the recently applied methods involves optical coherence tomography to measure retinal nerve fiber layer thickness in children with OPG.[43–45] In these studies, reduced ganglion cell-inner plexiform layer (GCL-IPL) thickness (<5th percentile) has been demonstrated to be an accurate surrogate marker of vision loss in children with OPG.[43,46] For this reason, we analyzed the retina in the 3 *Nf1* murine optic glioma strains at 3 months of age. Relative to control (FF) mice, FMC, FMBC, and FMPC mice exhibited an average 6-fold (range, 5.6%–6.9%) increase in RGC death (apoptosis; %TUNEL$^+$ cells; Fig. 4A and B) and an average 36% (range, 31%–45%) reduction

in RGC number (%Brn3a$^+$ cells; Fig. 4A and C). Using SMI-32 immunostaining (Fig. 4A), we next calculated the RNFL thickness as a function of the distance from the optic nerve head (Fig. 4D). We found an inverse correlation ($R^2 = 0.803$) between RGC death (TUNEL-positive cells) and RNFL thickness in all 3 mouse models, supporting that RNFL thinning results from loss of RGCs (Supplementary material, Fig. 2). While the 3 *Nf1* optic glioma mouse strains exhibited reduced RFNL thickness at all regions of the retina, FMPC mice had 3-fold reduced RNFL thickness proximate to the optic nerve head relative to control (FF) mice, compared with 2-fold reductions observed in FMC and FMBC mice in the same region.

Prior studies have shown that optic nerve axonal swelling and visual electrophysiological delays (visual evoked responses) precede RGC death in FMC mice,[47] such that restoring the reduced cyclic AMP levels in *Nf1+/−* neurons ameliorates the optic glioma-associated RGC apoptosis.[48] Based on these findings, we hypothesize that the larger, more proliferative FMPC optic gliomas result in greater retinal dysfunction that is initially more evident in the optic nerve head closer to the optic nerve axons. Since reduced visual acuity by virtual optokinetic system testing is not detected until 6 months of age in FMC mice,[49] future studies are in progress to compare the visual acuity deficits in these different *Nf1* optic glioma strains at older ages as well as to identify neuroprotective strategies to attenuate vision loss.

Collectively, these results reported herein demonstrate that *Pten* gene dose reduction, but not *KIAA1549:BRAF* expression, cooperates with neurofibromin loss to increase *Nf1* optic glioma growth and RGC dysfunction and further underscore the utility of GEM strains for defining the biological significance of genetic alterations discovered by advanced genomic analysis in human pathological specimens.

Supplementary Material

Supplementary material is available at Neuro-Oncology Journal online (http://neuro-oncology.oxfordjournals.org/).

Funding

Acknowledgments

Conflict of interest statement. None declared.

References

1. Gutmann DH, Aylsworth A, Carey JC, et al. The diagnostic evaluation and multidisciplinary management of neurofibromatosis 1 and neurofibromatosis 2. *JAMA*. 1997;278(1):51–57.

2. Sadighi Z, Slopis J. Pilocytic astrocytoma: a disease with evolving molecular heterogeneity. *J Child Neurol*. 2013;28(5):625–632.

3. Listernick R, Charrow J, Greenwald M, et al. Natural history of optic pathway tumors in children with neurofibromatosis type 1: a longitudinal study. *J Pediatr*. 1994;125(1):63–66.

4. Listernick R, Charrow J, Greenwald MJ, et al. Optic gliomas in children with neurofibromatosis type 1. *J Pediatr*. 1989;114(5):788–792.

5. Listernick R, Ferner RE, Liu GT, et al. Optic pathway gliomas in neurofibromatosis-1: controversies and recommendations. *Ann Neurol*. 2007;61(3):189–198.

6. Listernick R, Louis DN, Packer RJ, et al. Optic pathway gliomas in children with neurofibromatosis 1: consensus statement from the NF1 Optic Pathway Glioma Task Force. *Ann Neurol*. 1997;41(2): 143–149.

7. Habiby R, Silverman B, Listernick R, et al. Precocious puberty in children with neurofibromatosis type 1. *J Pediatr*. 1995;126(3): 364–367.

8. Sharif S, Ferner R, Birch JM, et al. Second primary tumors in neurofibromatosis 1 patients treated for optic glioma: substantial risks after radiotherapy. *J Clin Oncol*. 2006;24(16):2570–2575.

9. Mahoney DH Jr, Cohen ME, Friedman HS, et al. Carboplatin is effective therapy for young children with progressive optic pathway tumors: a Pediatric Oncology Group phase II study. *Neuro Oncol*. 2000;2(4): 213–220.

10. Packer RJ, Lange B, Ater J, et al. Carboplatin and vincristine for recurrent and newly diagnosed low-grade gliomas of childhood. *J Clin Oncol*. 1993;11(5):850–856.

11. Gutmann DH, McLellan MD, Hussain I, et al. Somatic neurofibromatosis type 1 (NF1) inactivation characterizes NF1-associated pilocytic astrocytoma. *Genome Res*. 2013;23(3):431–439.

12. Lau N, Feldkamp MM, Roncari L, et al. Loss of neurofibromin is associated with activation of RAS/MAPK and PI3-K/AKT signaling in a neurofibromatosis 1 astrocytoma. *J Neuropathol Exp Neurol*. 2000;59(9):759–767.

13. Gutmann DH, Donahoe J, Brown T, et al. Loss of neurofibromatosis 1 (NF1) gene expression in NF1-associated pilocytic astrocytomas. *Neuropathol Appl Neurobiol*. 2000;26(4):361–367.

14. Bajenaru ML, Hernandez MR, Perry A, et al. Optic nerve glioma in mice requires astrocyte Nf1 gene inactivation and Nf1 brain heterozygosity. *Cancer Res*. 2003;63(24):8573–8577.

15. Zhu Y, Harada T, Liu L, et al. Inactivation of NF1 in CNS causes increased glial progenitor proliferation and optic glioma formation. *Development*. 2005;132(24):5577–5588.

16. Bajenaru ML, Garbow JR, Perry A, et al. Natural history of neurofibromatosis 1-associated optic nerve glioma in mice. *Ann Neurol*. 2005;57(1):119–127.

17. Kim KY, Ju WK, Hegedus B, et al. Ultrastructural characterization of the optic pathway in a mouse model of neurofibromatosis-1 optic glioma. *Neuroscience*. 2010;170(1):178–188.

18. Rodriguez EF, Scheithauer BW, Giannini C, et al. PI3K/AKT pathway alterations are associated with clinically aggressive and histologically anaplastic subsets of pilocytic astrocytoma. *Acta Neuropathol*. 2011;121(3):407–420.

19. Rodriguez FJ, Ligon AH, Horkayne-Szakaly I, et al. BRAF duplications and MAPK pathway activation are frequent in gliomas of the optic nerve proper. *J Neuropathol Exp Neurol*. 2012;71(9):789–794.

20. Kaul A, Chen YH, Emnett R, et al. Conditional KIAA1549:BRAF mice reveal brain region- and cell type-specific effects. *Genesis*. 2013; 51(10):708–716.

21. Bajenaru ML, Zhu Y, Hedrick NM, et al. Astrocyte-specific inactivation of the neurofibromatosis 1 gene (NF1) is insufficient for astrocytoma formation. *Mol Cell Biol*. 2002;22(14):5100–5113.

22. Lesche R, Groszer M, Gao J, et al. Cre/loxP-mediated inactivation of the murine Pten tumor suppressor gene. *Genesis*. 2002;32(2):148–149.

23. Yeh TH, Lee da Y, Gianino SM, et al. Microarray analyses reveal regional astrocyte heterogeneity with implications for neurofibromatosis type 1 (NF1)-regulated glial proliferation. *Glia*. 2009;57(11):1239–1249.

24. Uhlmann EJ, Li W, Scheidenhelm DK, et al. Loss of tuberous sclerosis complex 1 (Tsc1) expression results in increased Rheb/S6 K pathway signaling important for astrocyte cell size regulation. *Glia*. 2004;47(2):180–188.

25. Lee DY, Gianino SM, Gutmann DH. Innate neural stem cell heterogeneity determines the patterning of glioma formation in children. *Cancer Cell*. 2012;22(1):131–138.

26. Kaul A, Chen YH, Emnett RJ, et al. Conditional KIAA1549:BRAF mice reveal brain region- and cell type-specific effects. *Genesis*. 2013;51(10):708–716.

27. Hegedus B, Banerjee D, Yeh TH, et al. Preclinical cancer therapy in a mouse model of neurofibromatosis-1 optic glioma. *Cancer Res*. 2008;68(5):1520–1528.

28. Hegedus B, Yeh TH, Lee da Y, et al. Neurofibromin regulates somatic growth through the hypothalamic-pituitary axis. *Hum Mol Genet*. 2008;17(19):2956–2966.

29. Jones DT, Kocialkowski S, Liu L, et al. Tandem duplication producing a novel oncogenic BRAF fusion gene defines the majority of pilocytic astrocytomas. *Cancer Res*. 2008;68(21):8673–8677.

30. Yu J, Deshmukh H, Gutmann RJ, et al. Alterations of BRAF and HIPK2 loci predominate in sporadic pilocytic astrocytoma. *Neurology*. 2009;73(19):1526–1531.

31. Gronych J, Korshunov A, Bageritz J, et al. An activated mutant BRAF kinase domain is sufficient to induce pilocytic astrocytoma in mice. *J Clin Invest*. 2011;121(4):1344–1348.

32. Gregorian C, Nakashima J, Dry SM, et al. PTEN dosage is essential for neurofibroma development and malinant transformation. *Proc Natl Acad Sci USA*. 2009;106(46):19479–19484.

33. Keng VW, Rahrmann EP, Watson AL, et al. PTEN and NF1 inactivation in Schwann cells produces a severe phenotype in the peripheral nervous system that promotes the development and malignant progression of peripheral nerve sheath tumors. *Cancer Res*. 2012;72(13):3405–3413.

34. Kwon CH, Zhao D, Chen J, et al. Pten haploinsufficiency accelerates formation of high-grade astrocytomas. *Cancer Res*. 2008;68(9):3286–3294.

35. Dasgupta B, Yi Y, Chen DY, et al. Proteomic analysis reveals hyperactivation of the mammalian target of rapamycin pathway in neurofibromatosis 1-associated human and mouse brain tumors. *Cancer Res*. 2005;65(7):2755–2760.

36. Banerjee S, Crouse NR, Emnett RJ, et al. Neurofibromatosis-1 regulates mTOR-mediated astrocyte growth and glioma formation in a TSC/Rheb-independent manner. *Proc Natl Acad Sci USA*. 2011;108(38):15996–16001.

37. Dasgupta T, Haas-Kogan DA. The combination of novel targeted molecular agents and radiation in the treatment of pediatric gliomas. *Front Oncol*. 2013;3:110.

38. Sunayama J, Sato A, Matsuda K, et al. Dual blocking of mTor and PI3K elicits a prodifferentiation effect on glioblastoma stem-like cells. *Neuro Oncol*. 2010;12(12):1205–1219.

39. Fisher MJ, Loguidice M, Gutmann DH, et al. Visual outcomes in children with neurofibromatosis type 1-associated optic pathway glioma following chemotherapy: a multicenter retrospective analysis. *Neuro Oncol*. 2012;14(6):790–797.

40. Isenberg JC, Templer A, Gao F, et al. Attention skills in children with neurofibromatosis type 1. *J Child Neurol*. 2013;28(1):45–49.

41. Garg S, Green J, Leadbitter K, et al. Neurofibromatosis type 1 and autism spectrum disorder. *Pediatrics*. 2013;132(6):e1642–e1648.

42. North KN, Riccardi V, Samango-Sprouse C, et al. Cognitive function and academic performance in neurofibromatosis. 1: consensus statement from the NF1 Cognitive Disorders Task Force. *Neurology*. 1997;48(4):1121–1127.

43. Avery RA, Hwang EI, Ishikawa H, et al. Handheld optical coherence tomography during sedation in young children with optic pathway gliomas. *JAMA Ophthalmol*. 2014;132(3):265–271.

44. Avery RA, Liu GT, Fisher MJ, et al. Retinal nerve fiber layer thickness in children with optic pathway gliomas. *Am J Ophthalmol*. 2011;151(3):542–549 e542.

45. Chang L, El-Dairi MA, Frempong TA, et al. Optical coherence tomography in the evaluation of neurofibromatosis type-1 subjects with optic pathway gliomas. *J AAPOS*. 2010;14(6):511–517.

46. Gu S, Glaug N, Cnaan A, et al. Ganglion cell layer-inner plexiform layer thickness and vision loss in young children with optic pathway gliomas. *Invest Ophthalmol Vis Sci*. 2014;55(3):1402–1408.

47. Hegedus B, Hughes FW, Garbow JR, et al. Optic nerve dysfunction in a mouse model of neurofibromatosis-1 optic glioma. *J Neuropathol Exp Neurol*. 2009;68(5):542–551.

48. Brown JA, Gianino SM, Gutmann DH. Defective cAMP generation underlies the sensitivity of CNS neurons to neurofibromatosis-1 heterozygosity. *J Neurosci*. 2010;30(16):5579–5589.

49. Diggs-Andrews KA, Brown JA, Gianino SM, et al. Sex Is a major determinant of neuronal dysfunction in neurofibromatosis type 1. *Ann Neurol*. 2014;75(2):309–316.